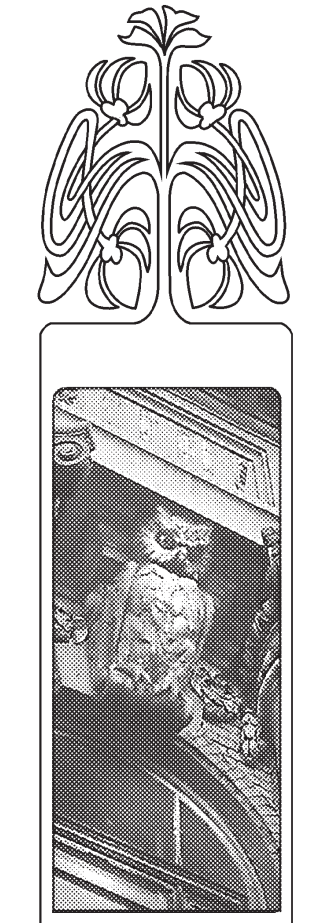

НАУЧНЫЙ ОТДЕЛ

РАДИОФИЗИКА, ЭЛЕКТРОНИКА, АКУСТИКА

Spiral Wave Patterns in Two-Layer 2D Lattices of Nonlocally Coupled Discrete Oscillators. Synchronization of Spiral Wave Chimeras

A. V. Bukh, G. I. Strelkova, V. S. Anishchenko

Andrei V. Bukh, https://orcid.org/0000-0002-4786-6157, Saratov State University, 83 Astrakhanskaya St., Saratov 410012, Russia, buh.andrey@yandex.ru

Galina I. Strelkova, https://orcid.org/0000-0002-8667-2742, Saratov State University, 83 Astrakhanskaya St., Saratov 410012, Russia, strelkovagi@info.sgu.ru

Vadim S. Anishchenko, https://orcid.org/0000-0003-2255-1498, Saratov State University, 83 Astrakhanskaya St., Saratov 410012, Russia, wadim@info.sgu.ru

The paper describes the spatio-temporal dynamics of a lattice that is given by a 2D $N \times N$ network of nonlocally coupled Nekorkin maps which model neuronal activity. The network behavior is studied for periodic and no-flux boundary conditions. It is shown that for certain values of the coupling parameters, rotating spiral waves and spiral wave chimeras can be observed in the considered lattice. We analyze and compare statistical and dynamical characteristics of the local oscillators from coherence and incoherence clusters of a spiral wave chimera. Furthermore, effects of mutual and external synchronization of spiral wave structures in two coupled such lattices are studied. We show numerically that spiral wave structures, including spiral wave chimeras, can be synchronized and establish the mechanism of their synchronization. Our numerical studies indicate that when the coupling strength between the lattices is sufficiently weak, only a certain part of oscillators of the interacting networks is imperfectly synchronized, while the other part demonstrates a partially synchronous behavior. If the spatiotemporal patterns in the lattices do not include incoherent cores, imperfect synchronization is realized for most oscillators above a certain value of the coupling strength. In the regime of spiral wave chimeras, the imperfect synchronization of all oscillators cannot be achieved even for sufficiently large values of the coupling strength.

Keywords: spiral waves, spiral wave chimera, networks, nonlocal coupling, discrete map, synchronization.

DOI: https://doi.org/10.18500/1817-3020-2019-19-3-166-177

1. Introduction

When studying the behavior of complex ensembles and networks of coupled nonlinear oscillators, the formation of various spatio-temporal patterns and their evolution are in the focus of research in nonlinear dynamics with applications to physics, chemistry, biology, and beyond [1–18].

In the last 15 years, the attention of specialists in nonlinear dynamics and related scientific fields was focused on the studies of so-called "chimera states" [19–22]. These states are characterized by the coexistence of clusters of oscillators with coherent (synchronous) and incoherent (asynchronous) dynamics in the ensemble space. Of particular interest is the synchronization of chimera states in multicomponent systems and

networks. Recently, various synchronization scenarios in multiplex and multilayer [23–31] networks were studied, such as generalized synchronization [32], inter-layer (external and mutual) synchronization [33–38], relay (remote) synchronization [39, 40], explosive synchronization [41–44]. Among a large variety of chimera states [35, 45–72], here we concentrate on so-called "spiral wave chimera structures" which are observed in 2D ensembles of coupled nonlinear oscillators [10, 22, 73–86]. These were typically found in the case of nonlocal coupling topology of network elements. These structures represent spiral waves which rotate around incoherent cores. The network elements in the regions of rotating spiral waves are characterized by coherent dynamics, while the elements inside the incoherent cores oscillate asynchronously. We note that spiral wave chimeras were observed in both numerical and experimental [78] studies of the dynamics of 2D ensembles whose individual oscillators are described, as a rule, by systems of ordinary differential equations.

In this paper we study the spatio-temporal dynamics of a 2D lattice of nonlocally coupled discrete-time systems. The network node is described by a two-dimensional nonlinear map proposed in the paper [87]. The Nekorkin map models the dynamics of a single neuron and can serve as a universal discrete model for describing the neuronal activity. During our numerical studies of the 2D lattice of coupled Nekorkin maps we observe spiral wave structures and spiral wave chimeras which are similar to those realized in ensembles of coupled phase or FitzHugh–Nagumo oscillators. It shoud be noted that simulating a large ensemble of coupled maps requires much less calculation time as compared with similar computations for ensembles of coupled differential systems. This circumstance is undoubtedly an important advantage which enables one to expand the area of computing and studying of complex networks of coupled oscillators.

In our work we consider two types of boundary conditions, periodic (torus) and no-flux (plane), and show that qualitatively, the results practically do not depend on their choice. In a spiral wave chimera regime, we analyze and compare dynamical and statistical characteristics of the network oscillators. Furthermore, effects of synchronization of spiral wave chimera structures have not been studied yet, and we describe numerical results for mutual and external synchronization of spiral wave structures in two coupled 2D lattices consisting of nonlocally coupled map-based neuron models [87].

2. Single Nekorkin map

Before focusing on the study of two coupled 2D lattices we describe briefly the dynamics of a single Nekorkin map which is a simple model for neuronal dynamics [87]. It is defined by the following equations:

$$\begin{aligned} x^{t+1} &= x^t + F\left(x^t\right) - y^t - \beta H\left(x^t - d\right), \\ y^{t+1} &= y^t + \varepsilon\left(x^t - J\right), \end{aligned} \tag{1}$$

where x^t is a variable that describes the dynamics of the membrane potential of the nerve cell, y^t is a variable that relates to the cumulative effect of all ion currents across the membrane, functions $F(x^t)$ and $H(x^t - d)$ are given as follows:

$$F\left(x^t\right) = x^t\left(x^t - a\right)\left(1 - x^t\right),\ 0 < a < 1, \tag{2}$$

$$H\left(x^t\right) = \left\{1, x^t > 0\right\} \vee \left\{0, \textit{elsewhere}\right\}. \tag{3}$$

The parameter ε determines the characteristic time scale of y^t, the parameter J controls the level of the membrane depolarization ($J < d$), the parameters $\beta > 0$ and $d > 0$ determine the excitation threshold of bursting oscillations, $t = 1,2,...$ represents discrete time. Despite its simplicity, this map can describe a number of basic modes of neuronal activity [88] when the control parameters are varied. These modes include spike-bursting chaotic oscillations, subthreshold oscillations, as well as the regime of single, periodic and chaotic spike generation [87].

In our studies we are especially interested in the dynamical regime of the map (1), which relates to spike oscillations. This mode is exemplified in Fig. 1, where the phase portrait and time series for the variable x^t are plotted respectively. The corresponding phase portrait represents a closed invariant curve. The maximal Lyapunov exponent in this regime is (up to numerical inaccuracy) zero, and the second one is negative. Thus, we can conclude that the map (1) dynamics reflects a quasi-periodic mode in a lifted continuous-time system [89]. However, as clearly seen from Fig. 1 *b*, the time series of the variable x^t is nearly periodic, and the rotation number for the invariant curve (Fig. 1 *a*) is very small, i.e., $r = 0.014$. In this case, the trajectory shifts on a very small angle per iteration that leads to the observation of nearly periodic oscillations and the invariant curve is very similar to a limit cycle. This fact is also confirmed by numerical results for the autocorrelation function. The latter decays gradually and very slowly as a consequence of nearly periodic oscillations (Fig. 1 *c*).

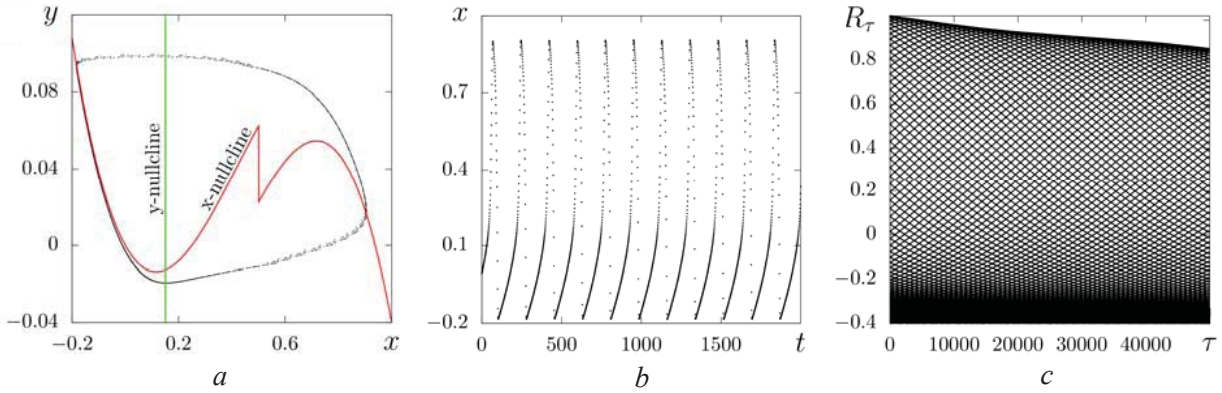

Fig. 1. (*a*) Phase portrait, (*b*) time series x^t and autocorrelation dependence (c) for the map (1) at $a = 0.25$, $\beta = 0.04$, $J = 0.15$, $d = 0.5$, $\varepsilon = 0.005$. The Lyapunov exponents are $\lambda_0 = 0.0$, $\lambda_1 = -0.4$, and the rotation number is $r = 0.014$

3. 2D lattice of coupled Nekorkin maps

We choose the Nekorkin map (1) as the individual element in a two-dimensional $N \times N$ lattice of nonlocally coupled oscillators. The network equations are as follows:

$$\begin{aligned} x_{i,j}^{t+1} &= x_{i,j}^t + F\left(x_{i,j}^t\right) - y_{i,j}^t - \beta H\left(x_{i,j}^t - d\right) + \\ &+ \frac{\sigma_x}{B_{i,j}^x} \sum \left[f\left(x_{m_x,n_x}^t\right) - f\left(x_{i,j}^t\right) \right], \\ y_{i,j}^{t+1} &= y_{i,j}^t + \varepsilon\left(x_{i,j}^t - J\right), \end{aligned} \tag{4}$$

where m_x, $n_x \in$ are indices for nonlocal neighbors. The sum denotes nonlocal coupling of range R_x in a square domain. The network (4) is analyzed for both periodic

$$\begin{aligned} &i - R_x \le m_x \le i + R_x, \ i \pm N = i, \\ &j - R_x \le n_x \le N, \ j + R_x, \ j \pm N = j, \end{aligned} \tag{5}$$

and no-flux [90]

$$\begin{aligned} &\max\left(1, i - R_x\right) \le m_x \le \min\left(N, i + R_x\right), \\ &\max\left(1, j - R_x\right) \le n_x \le \min\left(N, j + R_x\right). \end{aligned} \tag{6}$$

boundary conditions. The double index of variables $x_{i,j}$ and $y_{i,j}$ with $i, j = 1, \ldots, N$ encodes the position of corresponding oscillators on the two-dimensional lattice. The parameter σ_x denotes the coupling strength between the elements in the x variable $B_{i,j}^x$ gives the number of nonlocally coupled neighbors of node (i, j). In the case of periodic boundary conditions, we have $B_{i,j}^x = \left(2R_x + 1\right)^2 - 1$. The numerical results show that when the nonlocal coupling strength σ_x and the coupling range R_x are varied, the model (4) can demonstrate all the typical spiral wave patterns, including spiral wave chimeras, which were observed earlier.

The dynamics of the network (4) is analyzed when the individual element (the map (1)) operates in the spike oscillation mode (Fig. 1). In our simulations we use initial conditions randomly and uniformly distributed in the intervals $x_{i,j}^0 \in [-0.2, 0.6]$, $y_{i,j}^0 \in [-0.02, 0.06]$. Examples of spatio-temporal patterns which arise in the network (4) of locally coupled maps, i.e., when $R_x = 1$, are shown in Fig. 2 for increasing values of the coupling strength σ_x and for two types of boundary conditions. The upper panel shows snapshots of $x_{i,j}$ in the case of no-flux boundary conditions (5) and the lower panel depicts snapshots of $x_{i,j}$ for periodic boundary conditions (6). The coupling strength σ_x takes the same values for both cases. When σ_x is very weak, e.g., $\sigma_x = 0.0001$, the individual elements behave as if they are uncoupled. An incoherent mode with small coherence clusters is realized at rather small values of σ_x (see, for example, Fig. 2 *a*, *d* at $\sigma_x = 0.003$). When the coupling strength increases and becomes sufficiently strong, e.g., $\sigma_x = 0.027$, smooth coherent patterns are observed in the lattice (Fig. 2 *c*, *f*). Spiral wave structures are found in the network when σ_x takes intermediate values. Examples are depicted in Fig. 2 *b*,*e* for $\sigma_x = 0.018$. As can be seen from Fig. 2, the obtained patterns do not dramatically differ from each other for different types of boundary conditions.

We now explain how we obtain spatio-temporal patterns in the network (4) when the coupling parameters are varied. We use random initial conditions as specified above. Whenever we observe a spiral wave

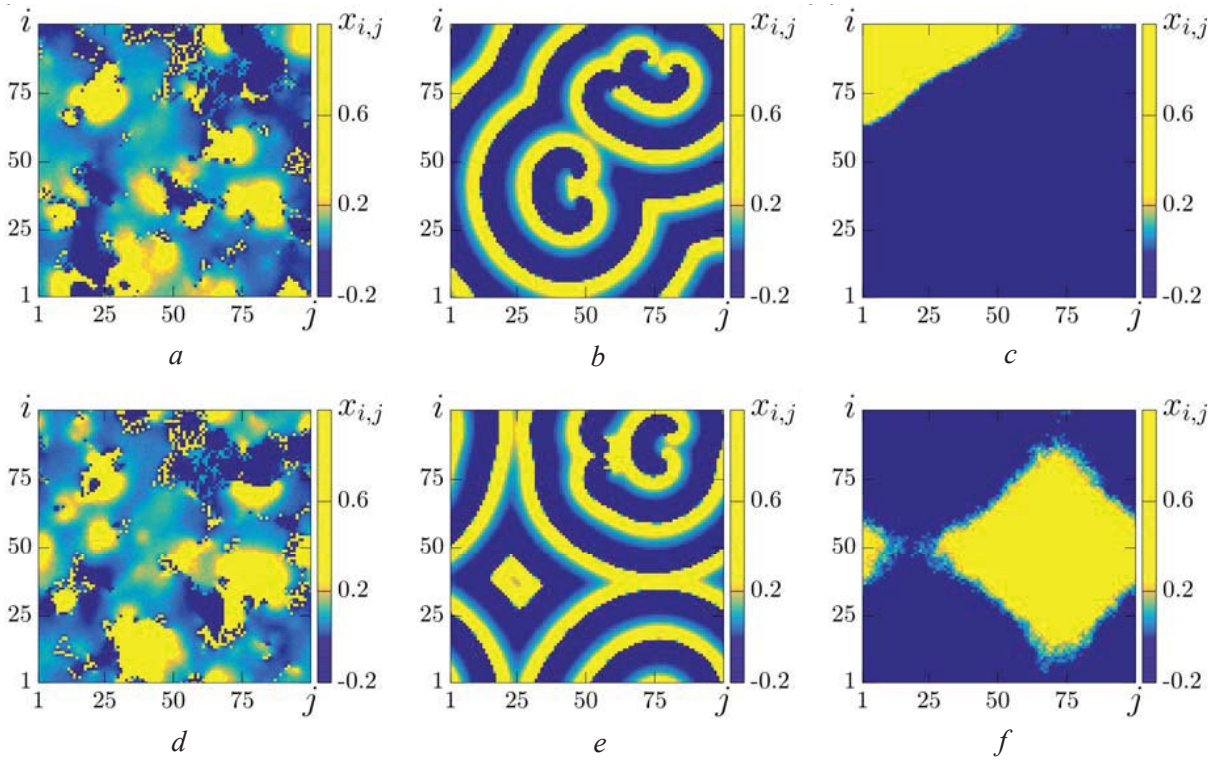

Fig. 2. Snapshots of the $x^t_{i,j}$ variable in the network (4) for different values of the coupling strength σ_x: (*a*, *d*) 0.003, (*b*, *e*) 0.018, (*c*, *f*) 0.027. The upper and lower panels depict snapshots for no-flux and periodic boundary conditions, respectively. Other parameters: $a = 0.25$, $\beta = 0.04$, $J = 0.15$, $d = 0.5$, $\varepsilon = 0.004$ and $R_x = 1$

pattern for the coupling range $R_x = 1$, we continue our calculation by changing the coupling parameters using the pattern of the previous simulation as an initial condition. Our calculations show that the observed spatio-temporal patterns strongly depend on the coupling range. Examples are shown in Fig. 3 for different values of R_x and a fixed value of σ_x in the case of no-flux boundaries. Following our calculation scheme described above, we observe the spatio-temporal pattern at $R_x = 1$ and $\sigma_x = 0.05$ (Fig. 3 *a*) and then increase the coupling range R_x. When $R_x = 6$, the incoherent core appears near the lattice center and is surrounded by the rotating spiral wave (Fig. 3 *b*). This means that a spiral wave chimera state is observed. A further increase in the coupling range leads to an increase of the size of the incoherent core (Fig. 3 *c*), which is now strictly located at the lattice center.

Spiral wave patterns and spiral wave chimeras can also be found for periodic boundary conditions when the coupling range R_x increases. The number of incoherent cores also increases as R_x goes up (Fig. 4).

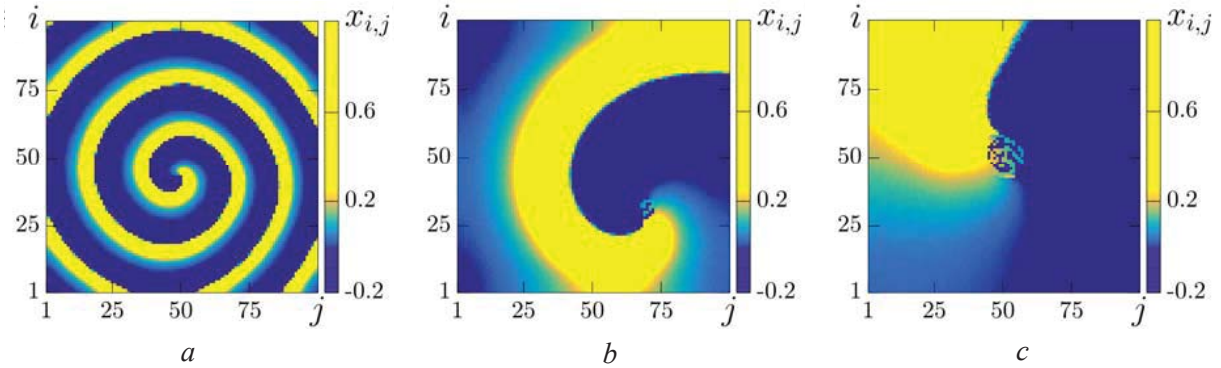

Fig. 3. Spiral wave pattern and spiral wave chimeras in the lattice (4) for no-flux boundaries. Snapshots of $x^t_{i,j}$ for increasing values of the coupling range: (*a*) $R_x = 1$, (*b*) $R_x = 6$, (*c*) $R_x = 14$. Other parameters: $a = 0.25$, $\beta = 0.04$, $J = 0.15$, $d = 0.5$, $\varepsilon = 0.004$ and $\sigma_x = 0.05$

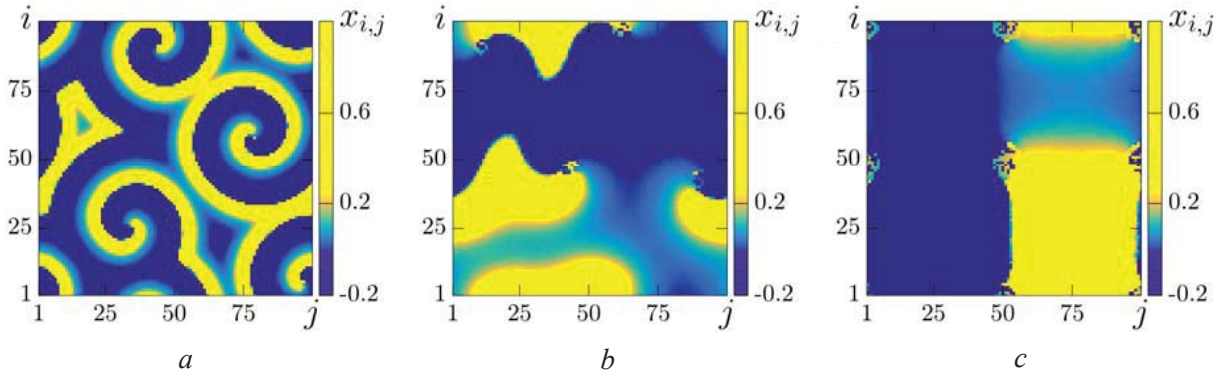

Fig. 4. Spiral wave pattern and spiral wave chimeras with several incoherent cores in the network (4) for periodic boundary conditions. Snapshots of $x^t_{i,j}$ for increasing values of the coupling range: (*a*) $R_x = 1$, (*b*) $R_x = 5$, (*c*) $R_x = 12$. Other parameters: $a = 0.25$, $\beta = 0.04$, $J = 0.15$, $d = 0.5$, $\varepsilon = 0.004$ and $\sigma_x = 0.05$

4. Two coupled 2D lattices of Nekorkin maps

We now couple two 2D lattices each described by the network (4) of 200 × 200 nonlocally coupled Nekorkin maps. The coupling between the lattices is assumed to be mutual. This means that only corresponding oscillators of the lattices are mutually coupled via their coordinates, i.e., in a multiplex configuration. In this case the coupled lattices are described by the following system of equations:

$$\begin{aligned}
x^{t+1}_{i,j} &= x^t_{i,j} + F\left(x^t_{i,j}\right) - y^t_{i,j} - \beta H\left(x^t_{i,j} - d\right) + \frac{\sigma_x}{B^x_{i,j}} \sum \left[f\left(x^t_{m_x,n_x}\right) - f\left(x^t_{i,j}\right) \right] + \gamma_{ux}\left[u^t_{i,j} - x^t_{i,j}\right], \\
y^{t+1}_{i,j} &= y^t_{i,j} + \varepsilon\left(x^t_{i,j} - J\right), \\
u^{t+1}_{i,j} &= u^t_{i,j} + F\left(u^t_{i,j}\right) - v^t_{i,j} - \beta H\left(u^t_{i,j} - d\right) + \frac{\sigma_u}{B^u_{i,j}} \sum \left[f\left(x^t_{m_u,n_u}\right) - f\left(u^t_{i,j}\right) \right] + \gamma_{xu}\left[x^t_{i,j} - u^t_{i,j}\right], \\
v^{t+1}_{i,j} &= v^t_{i,j} + \varepsilon\left(u^t_{i,j} - J\right),
\end{aligned} \tag{7}$$

where variables $x^t_{i,j}$, $y^t_{i,j}$ define the dynamics of the oscillators in the first lattice, variables $u^t_{i,j}$, $v^t_{i,j}$ determine the dynamics of the oscillators in the second lattice, γ_{ux}, γ_{xu}, are the interlattice coupling strengths between corresponding oscillators of the first and second lattice layer. In our studies we consider only the case of no-flux boundary conditions. Link indices $m_x, n_x \in$ are given in Eq. (6) for the first lattice, and indices $m_u, n_u \in$ in the second lattice are defined analogously by replacing R_x, with R_u. To account for potentially different coupling parameters in both networks, we introduce a subscript x and u for the first and second network in the coupling strengths σ_x, σ_u, coupling ranges R_x, R_u, numbers of nonlocal neighbors $B^x_{i,j}$, $B^u_{i,j}$ and neighbor indices m_x, m_u, n_x, n_u. The values of the coupling strengths are fixed as $\sigma_x = \sigma_u = 0.6$.

The synchronization of oscillations between the lattices is quantified by calculating the number of synchronized elements N_s in the lattices, which satisfy the condition $r_{i,j} \geq 0.95$, where the correlation coefficient $r_{i,j}$ between corresponding oscillators of the lattices is given as follows:

$$r_{i,j} = \frac{\tilde{x}_{i,j}\tilde{u}_{i,j}}{\sqrt{\tilde{x}^2_{i,j}\,\tilde{u}^2_{i,j}}}, \qquad \tilde{x}_{i,j} = x_{i,j} - \langle x_{i,j} \rangle, \tilde{u}_{i,j} = u_{i,j} - \langle u_{i,j} \rangle. \tag{8}$$

The correlation coefficient $r_{i,j}$ is widely used when synchronization of coupled oscillators is studied [60, 91]. The corresponding oscillators are assumed to be synchronized if $r_{i,j} \geq 0.95$, otherwise they are desynchronized. The threshold value of $r^{th}_{i,j} = 0.95$ is chosen because complete synchronization cannot be achieved in the case of parameter detuning in the interacting lattices. The condition $r_{i,j} \geq 0.95$, characterizes the maximum degree of synchronization of spatio-temporal structures which is possible in the regimes studied.

5. Numerical results for mutual synchronization

The parameters of the individual map (1) are set as in Section II. The coupling strengths between the lattices are assumed to be $\gamma_{ux} = \gamma_{xu} = \gamma$ in the case of mutual synchronization. We consider the dynamics of the coupled lattices (7) when the coupling strength γ is varied. In our simulations spatio-temporal patterns in the network (4) are obtained as follows. We use random initial conditions distributed in the intervals $x^0_{i,j}, u^0_{i,j} \in [-0.2, 0.6]$, $y^0_{i,j}, v^0_{i,j} \in [-0.02, 0.06]$ for the coupling range $R_x = R_u = 1$. Whenever we observe a spiral wave pattern in each uncoupled lattice at $R_x = R_u = 1$, we use this as initial condition and continue our calculation by changing the coupling parameters. First, we choose simple but non-identical spiral wave structures which are realized in the lattices when they are uncoupled. These patterns are exemplified in Fig. 5 *a, b*. As can be seen from Fig. 5 *c*, when the mutual coupling γ is turned on, the resulting structure in the network (7) differs from the initial patterns in both lattices (Fig. 5 *a*, *b*) and represents a certain intermediate regime due to the mutual coupling which is invasive. The topology of this spiral wave structure is preserved, but the wavelength of the spiral wave in Fig. 5 *c* does not coincide with that of the initial structures (Fig. 5 *a*, *b*). We measure the wavelength for each pattern by taking a cross section through the spiral center and then compare the wavelengths.

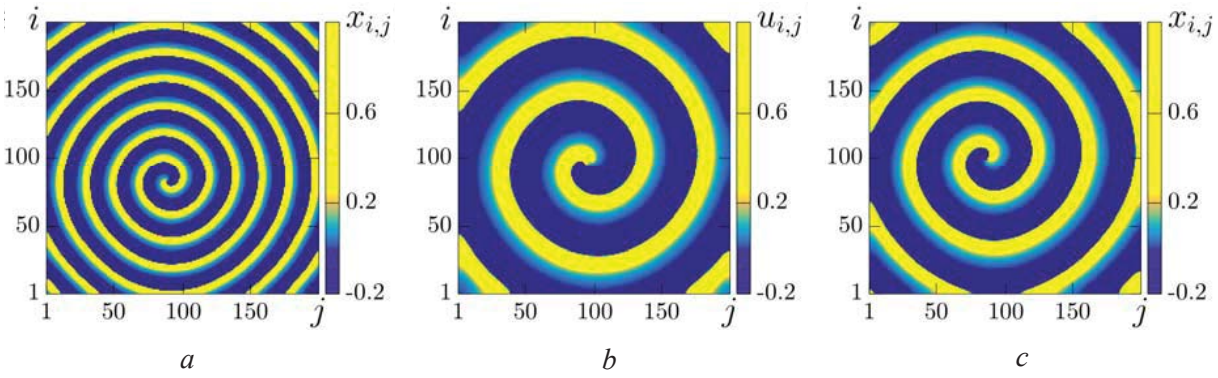

Fig. 5. Snapshots of (*a*) $x_{i,j}$ (first lattice) for $R_x = 1$, $\gamma = 0$ (b) $u_{i,j}$ (second lattice) at $R_u = 3$, $\gamma = 0$, (c) $x_{i,j}$ (first lattice) for $\gamma = 0.04$. Other parameters as in Fig. 1

Our calculations show that different oscillators in the lattices are synchronized at different values of the interlattice coupling strength γ. As follows from Fig. 6 *a*, when the coupling strength is rather weak, $\gamma \le 0.02$, none of the oscillators ($N_s = 0$) are in-phase synchronized. This is well illustrated by the distribution of the correlation coefficient $r_{i,j}$ shown in Fig. 6 *b*. Synchronization is observed only with

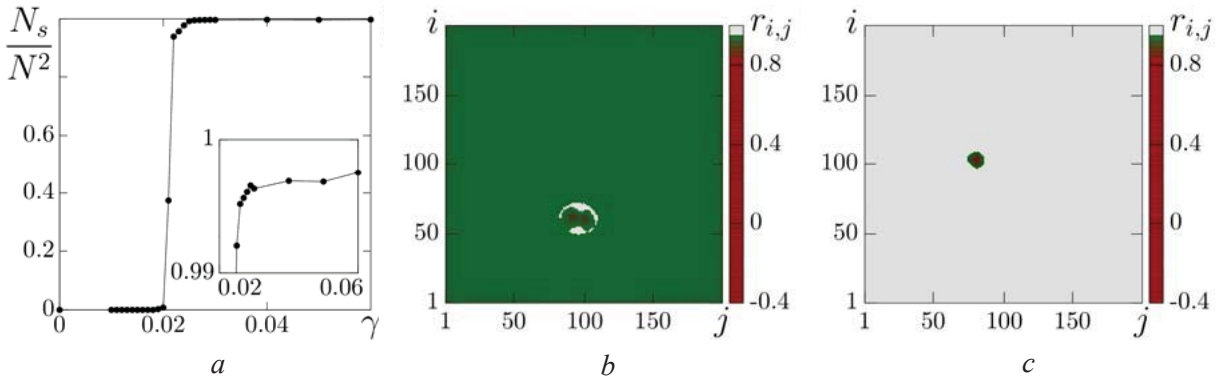

Fig. 6. (*a*) Number of synchronous oscillators $\left(\{N_s : r_{i,j} > 0.95\}\right)$ versus the interlattice coupling strength γ, distribution of the correlation coefficient $r_{i,j}$ at (b) $\gamma = 0.02$, (c) $\gamma = 0.04$ with $R_x = 1$, $R_u = 3$. Coherent oscillators (i, j) are marked by the light tone (grey online), incoherent ones by the dark tone (green or red online). The inset in (*a*) shows a blow-up for N_s / N^2 close to unity

$\gamma > 0.02$ and most oscillators are synchronized at $\gamma = 0.03$. However, the distribution of the correlation coefficient $r_{i,j}$ depicted in Fig. 6 *c* clearly indicates that there is a certain number of desynchronized oscillators which are located in the center of the lattices. For these oscillators the correlation coefficient $r_{i,j} < 0.9$. Hence, we can state that partial synchronization takes place in this case. The regime of partial synchronization is characterized by the coexistence of synchronous and asynchronous oscillators in the interacting lattices. As can be seen from Figs. 5 *c*, 6 *c*, the asynchronous oscillators correspond to the core of the spiral wave. Almost complete synchronization of all elements is achieved when $\gamma > 0.05$.

We now consider mutual synchronization of a coherent spiral wave and a spiral wave chimera with single core pictured in Fig. 7. Numerical calculations show that the topology of spiral wave structures essentially depends on the coupling ranges R_x and R_u. Particularly, the number of incoherent cores changes when R_x and R_u are varied. When the lattices are uncoupled, a spiral wave pattern is realized in the first lattice (Fig. 7 *a*) and a spiral wave chimera is observed in the second one (Fig. 7 *b*). The synchronous structure which results from the mutual synchronization of the two coupled lattices (7) is presented in Fig. 7 *c*. Our numerical results indicate that the effect of partial synchronization manifests itself more brightly in this case. Moreover, as follows from Fig. 8 *a*, a larger interlattice coupling strength $\gamma \geq 0.04$ is needed to synchronize most of the oscillators in the lattices. At the same time, the number of oscillators which remain desynchronized increases (Fig. 8 *c*) as compared with Fig. 6 *c*. The distribution of the correlation coefficient $r_{i,j}$ values for the transient structure at $\gamma = 0.02$ is shown in Fig. 8 *b*. A comparison of the results presented in Figs. 5, 6 and Figs. 7, 8 shows that the number of desynchronized oscillators increases when the incoherent core appears.

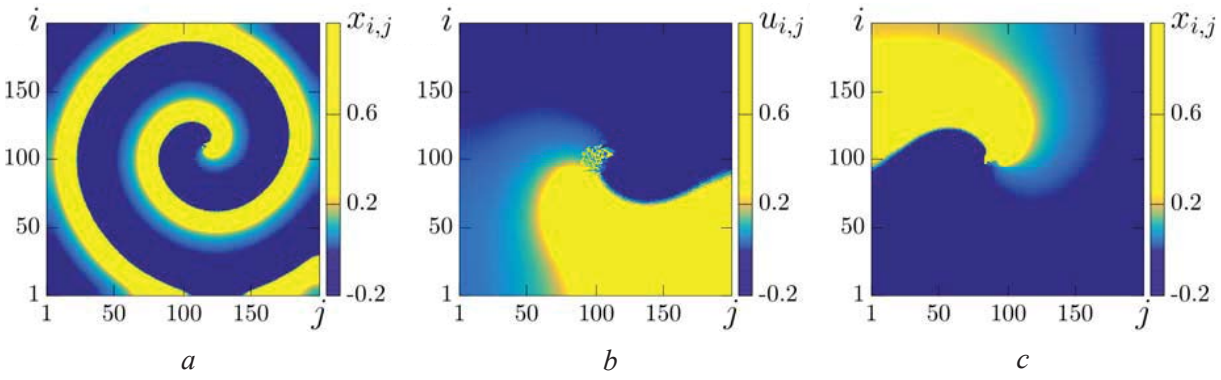

Fig. 7. Snapshots of (*a*) $x_{i,j}$ (first lattice) for $R_x = 4$, $\gamma = 0$, (*b*) $u_{i,j}$ (second lattice) at $R_u = 22$, $\gamma = 0$, (*c*) $x_{i,j}$ (first lattice) for $\gamma = 0.06$

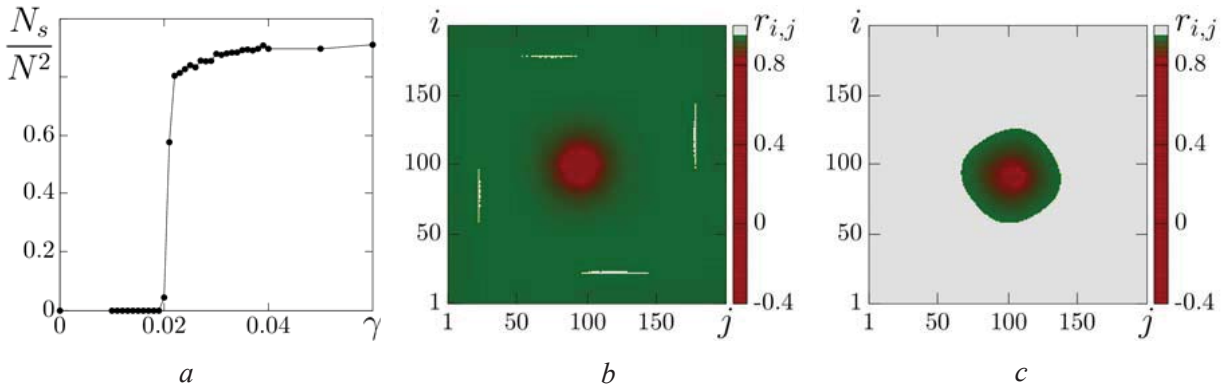

Fig. 8. (*a*) Number of synchronous oscillators $\left(\left\{N_s : r_{i,j} > 0.95\right\}\right)$ in dependence on the interlattice coupling strength γ, distribution of the $r_{i,j}$ values at (*b*) $\gamma = 0.02$, (*c*) $\gamma = 0.06$ with $R_x = 4$, $R_u = 22$

6. Numerical results for external synchronization

We now analyze the case of external synchronization when the interlattice coupling is introduced unidirectionally from the elements of the second lattice, which is the driver network, to the corresponding elements of the first lattice, which is the response network. Thus, we set $\gamma_{ux} = \gamma, \gamma_{xu} = 0$ in (7). The results of numerical simulations are shown in Figs. 9–10 for two different spiral wave chimera structures realized in the driver lattice. When the lattices are uncoupled, a spiral wave chimera is established in the second (driver) lattice (Fig. 9 *b*) and a coherent spiral wave is realized in the first (response) lattice (Fig. 9 *a*). The partial external synchronization which takes place in the coupled lattices starting with $\gamma \geq 0.05$ (Fig. 10 *a*) results in the synchronous state shown in Fig. 9 *c*. However, as can be seen from Fig. 10 *c*, the oscillators in the incoherent core of the spiral wave chimera (in the center of the lattice in Fig. 9 *c*) are desynchronized and this feature is preserved for sufficiently large values of $\gamma \geq 0.02$. Moreover, the incoherent core corresponds exactly to the incoherent core in the resulting synchronous pattern (Fig. 9 *c*). The number of desynchronized oscillators grows when the number of incoherent cores increases. Our numerical studies have shown that this effect is general for both mutual and external synchronization.

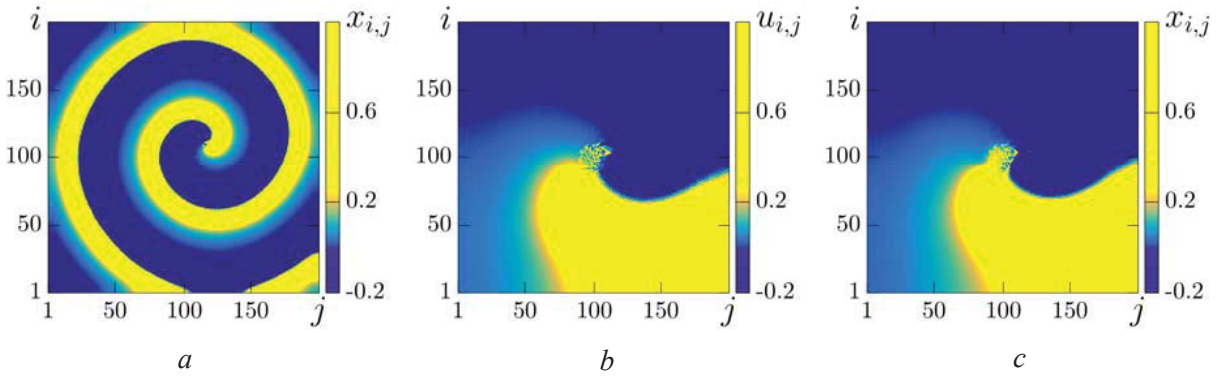

Fig. 9. Snapshots of (*a*) $x_{i,j}$ in the first (response) lattice at $R_x = 4$, $\gamma = 0$, (*b*) $u_{i,j}$ in second (driver) lattice at $R_u = 22$, $\gamma = 0$, (*c*) $x_{i,j}$ in the response lattice for $\gamma = 0.05$

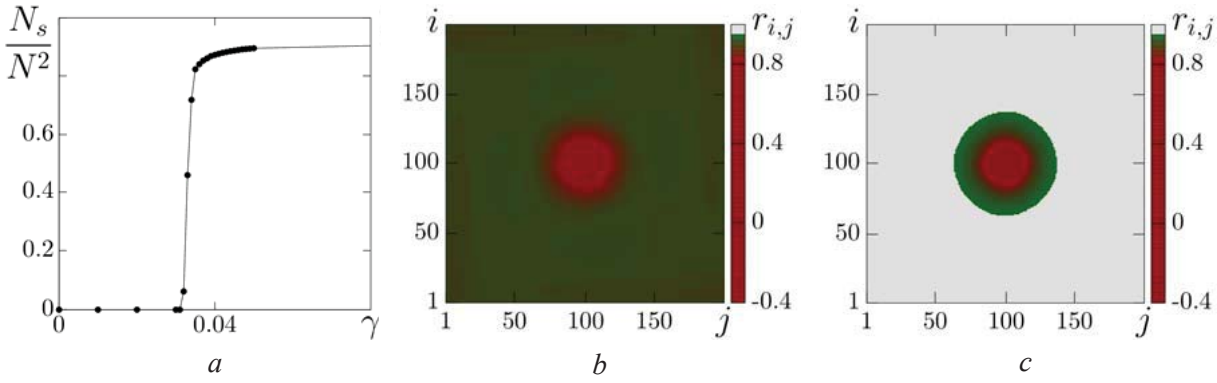

Fig. 10. (*a*) Number of synchronous oscillators $\left(\{N_s : r_{i,j} > 0.95\}\right)$ versus the unidirectional interlattice coupling strength γ, distribution of the $r_{i,j}$ values at (*b*) $\gamma = 0.02$, (*c*) $\gamma = 0.05$ with $R_x = 4$, $R_u = 22$

7. Conclusions

We have studied the dynamics of a two-dimensional network of discrete-time maps with nonlocal interaction. The local dynamics of the network element is defined by the Nekorkin map which is a universal discrete model of the neuronal activity. This map can describe a variety of different dynamical modes, including chaotic spike-bursting oscillations, subthreshold and spike oscillations.

We have shown for the first time that the 2D lattice of coupled map-based neuron models can demonstrate all typical spatio-temporal structures,

including spiral wave patterns and spiral wave chimeras, which are similar to those observed in 2D networks of nonlocally coupled phase oscillators, FitzHugh–Nagumo models, reaction-diffusion models, chemical oscillators, etc. The network dynamics has been explored for two types of boundary conditions, periodic (toroidal) and no-flux (plane) and it has been shown that the resulting patterns have not changed qualitatively depending on the choice of boundary conditions. Our studies have demonstrated that the spiral wave chimeras can be observed within finite ranges of variation of the nonlocal coupling paratemers and the multi-core chimeras can be obtained when the coupling range R_x increases.

Our numerical studies have convicingly shown that a simple discrete-time system in the form of the Nekorkin map, that describes well a rich variety of the neuronal activity, can be chosen and used as individual element of a complex network for further extended analysis of the properties and characteristics of spiral wave patterns and spiral wave chimeras. We have analyzed numerically the mutual and external synchronization of two coupled lattices consisting of nonlocally coupled Nekorkin maps. Our numerical studies have shown that these synchronization effects are characterized by several important features. First, if each of the uncoupled lattices exhibits simple spiral wave structures, imperfect (almost complete) synchronization of oscillations of most corresponding elements of the two lattices can occur for a sufficient value of the coupling strength γ. We note that in the case of mutual synchronization, the resulting synchronous structure differs from the initially established modes in the uncoupled lattices. This effect is typical and has also been encountered when mutual synchronization of two oscillators with limit cycles [92] was considered. Complete synchronization cannot be achieved even with a significant increase in the coupling strength, if one of the lattices exhibits a spiral wave chimera pattern for zero interlattice coupling. The second peculiarity consists of the fact that not all oscillators are almost completely synchronized when the lattices are coupled mutually or unidirectionally. A certain number of oscillators remain desynchronized while most of them demonstrate imperfect (almost complete) synchronization. This effect takes place even in the case of simple (single-core) initial patterns in both lattices and is enhanced when the initial spiral wave chimera in one of the interacting lattices has multiple cores. It has been shown that the transition from a spiral wave chimera structure with a single core to a spiral wave chimera with several cores is characterized by an increase in the number of unsynchronized oscillators.

Acknowledgements: *This work was funded by the Deutsche Forschungsgemeinschaft (DFG, German Research Foundation) – Projektnummer 163436311-SFB 910, and by the Russian Ministry of Education and Science (project No. 3.8616.2017).*

References

1. Kaneko K. Pattern dynamics in spatiotemporal chaos. *Physica D*, 1967, vol. 34, pp. 1–41.
2. Afraimovich V., Nekorkin V., Osipov G., Shalfeev V. *Stability, Structures And Chaos In Nonlinear Synchronization Networks.* Singapore, World Scientific, 1995. 260 p.
3. Epstein I. R., Pojman J. A. *An introduction to nonlinear chemical dynamics: oscillations, waves, patterns, and chaos*. Oxford, Oxford University Press, 1998. 480 p.
4. Strogatz S. H. Exploring complex networks. *Nature*, 2001, vol. 410, pp. 268.
5. Nekorkin V. I., Velarde M. G. *Synergetic Phenomena in Active Lattices*. Berlin, Springer, 2002. 359 p.
6. Dorogovtsev S. N., Mendes J. F. Evolution of networks. *Advances in physics*, 2002, vol. 51, pp. 1079–1187.
7. Newman M. E. The structure and function of complex networks. *SIAM review*, 2003, vol. 45, pp. 167–256.
8. Ben-Naim E., Frauenfelder H., Toroczkai Z. *Complex networks.* Berlin, Springer, 2004. 520 p.
9. Boccaletti S., Latora V., Moreno Y., Chavez M., Hwang D.-U. Complex networks: Structure and dynamics. *Physics reports*, 2006, vol. 424, pp. 175–308.
10. Martens E. A., Laing C. R., Strogatz S. H. Solvable model of spiral wave chimeras. *Phys. Rev. Lett.*, 2010, vol. 104, pp. 044101.
11. Barabási A.-L., Pósfai M. Network science. Cambridge, Cambridge University Press, 2016. 475 p.
12. Pecora L. M., Sorrentino F., Hagerstrom A. M., Murphy T. E., Roy R. Cluster synchronization and isolated desynchronization in complex networks with symmetries. *Nat. Commun.*, 2014, vol. 5, pp. 4079.
13. Nekorkin V. I., Kazantsev V. B., Velarde M. G. Mutual synchronization of two lattices of bistable elements. *Phys. Lett. A*, 1997, vol. 236, pp. 505–512.
14. Nekorkin V. I., Voronin M. L., Velarde M. G. Clusters in an assembly of globally coupled bistable oscillators. *Eur. Phys. J. B*, 1999, vol. 9, pp. 533–543.
15. Belykh V. N., Belykh I. V., Hasler M. Hierarchy and stability of partially synchronous oscillations of diffusively coupled dynamical systems. *Phys. Rev. E*, 2000, vol. 62, pp. 6332–6345.

16. Belykh V. N., Belykh I. V., Mosekilde E. Cluster synchronization modes in an ensemble of coupled chaotic oscillators. *Phys. Rev. E*, 2001, vol. 63, pp. 036216.
17. Nekorkin V., Kazantsev V., Velarde M. Synchronization in two-layer bistable coupled map lattices. *Physica D*, 2001, vol. 151, pp. 1–26.
18. Akopov A., Astakhov V., Vadivasova T., Shabunin A., Kapitaniak T. Frequency synchronization of clusters in coupled extended systems. *Phys. Lett. A*, 2005, vol. 334, pp. 169–172.
19. Hogan J., Krauskopf A. R., Bernado M. di, Wilson R. E., Osigna H. M., Homer M. E., Champneys A. R. *Nonlinear Dynamics and Chaos. Where do we go from here?* Florida, US, CRC Press, 2002. 376 p.
20. Kuramoto Y., Battogtokh D. Coexistence of coherence and incoherence in nonlocally coupled phase oscillators. *Nonlinear Phenom. Complex Syst.*, 2002, vol. 5, pp. 380–385.
21. Abrams D. M., Strogatz S. H. Chimera states for coupled oscillators. *Phys. Rev. Lett.*, 2004, vol. 93, pp. 174102.
22. Panaggio M. J., Abrams D. M. Chimera states: coexistence of coherence and incoherence in networks of coupled oscillators. *Nonlinearity*, 2015, vol. 28, pp. R67–R87.
23. Domenico M. De, Solé-Ribalta A., Cozzo E., Kivelä M., Moreno Y., Porter M. A., Gómez S., Arenas A., Mathematical formulation of multilayer networks. *Phys. Rev. X*, 2013, vol. 3, pp. 041022.
24. Kivel M., Arenas A., Barthelemy M., Gleeson J. P., Moreno Y., Porter M. A. Multilayer networks. *J. Complex Netw.*, 2014, vol. 2, pp. 203–271.
25. Boccaletti S., Bianconi G., Criado R., Genio C. del, Gmez-Gardees J., Romance M., Sendia-Nadal I., Wang Z., Zanin M. The structure and dynamics of multilayer networks. *Phys. Rep.*, 2014, vol. 544, pp. 1 – 122.
26. Gambuzza L. V., Frasca M., Gómez-Gardeñes J. Intralayer synchronization in multiplex networks. *Europhys. Lett.*, 2015, vol. 110, pp. 20010.
27. Ghosh S., Kumar A., Zakharova A., Jalan S. Birth and death of chimera: Interplay of delay and multiplexing. *Europhys. Lett.*, 2016, vol. 115, pp. 60005.
28. Sevilla-Escoboza R., Sendia-Nadal I., Leyva I., Gutirrez R., Buld J. M., Boccaletti S. Inter-layer synchronization in multiplex networks of identical layers. *Chaos*, 2016, vol. 26, pp. 065304.
29. Ghosh S., Jalan S. Emergence of chimera in multiplex network. *Int J Bifurc Chaos,* 2016, vol. 26, pp. 1650120.
30. Maksimenko V. A., Makarov V. V., Bera B. K., Ghosh D., Dana S. K., Goremyko M. V., Frolov N. S., Koronovskii A. A., Hramov A. E. Excitation and suppression of chimera states by multiplexing. *Phys. Rev. E*, 2016, vol. 94, pp. 052205.
31. Mikhaylenko M., Ramlow L., Jalan S., Zakharova A. Weak multiplexing in neural networks: Switching between chimera and solitary states. *Chaos*, 2019, vol. 29, pp. 023122.
32. Andrzejak R. G., Ruzzene G., Malvestio I. Generalized synchronization between chimera states. *Chaos*, 2017, vol. 27, pp. 053114.
33. Singh A., Ghosh S., Jalan S., Kurths J. Synchronization in delayed multiplex networks. *Europhys. Lett.,* 2015, vol. 111, pp. 30010.
34. Boccaletti S., Almendral J., Guan S., Leyva I., Liu Z., Sendia-Nadal I., Wang Z., Zou Y. Explosive transitions in complex networks structure and dynamics: Percolation and synchronization. *Phys. Rep.*, 2016, vol. 660, pp. 1 – 94.
35. Bukh A., Rybalova E., Semenova N., Strelkova G., Anishchenko V., New type of chimera and mutual synchronization of spatiotemporal structures in two coupled ensembles of nonlocally interacting chaotic maps. *Chaos*, 2017, vol. 27, pp. 111102.
36. Bukh A. V., Strelkova G. I., Anishchenko V. S. Synchronization of chimera states in coupled networks of nonlinear chaotic oscillators. *Russ. J. Nonlin. Dyn.*, 2018, vol. 14, pp. 419–433.
37. Strelkova G., Vadivasova T., Anishchenko V. Synchronization of chimera states in a network of many unidirectionally coupled layers of discrete maps. *Regul. Chaot. Dyn.*, 2018, vol. 23, pp. 948 – 960.
38. Rybalova E., Vadivasova T., Strelkova G., Anishchenko V., Zakharova A. Forced synchronization of a multilayer heterogeneous network of chaotic maps in the chimera state mode. *Chaos*, 2019, vol. 29, pp. 033134.
39. Leyva I., Sevilla-Escoboza R., Sendia-Nadal I., Gutirrez R., Buld J., Boccaletti S. Inter-layer synchronization in non-identical multi-layer networks. *Sci. Rep.*, 2017, vol. 7, pp. 45475.
40. Sawicki J., Omelchenko I., Zakharova A., Schöll E. Delay controls chimera relay synchronization in multiplex networks. *Phys. Rev. E*, 2018, vol. 98, pp. 062224.
41. Zhang X., Boccaletti S., Guan S., Liu Z. Explosive synchronization in adaptive and multilayer networks. *Phys. Rev. Lett.*, 2015, vol. 114, pp. 038701.
42. Leyva I., Sendia-Nadal I., Sevilla-Escoboza R., Vera-Avila V. P., Chholak P., Boccaletti S. Relay synchronization in multiplex networks. *Sci. Rep.*, 2018, vol. 8, pp. 8629.
43. Leyva I., Sendia-Nadal I., Boccaletti S. Explosive synchronization in mono and multilayer networks. *Disc. and Cont. Dyn. Syst. Ser. B*, 2018, vol. 25, pp. 1931.
44. Kachhvah A. D., Jalan S. Delay regulated explosive synchronization in multiplex networks. *New J. Phys.*, 2019, vol. 21, pp. 015006.
45. Omelchenko I., Maistrenko Y., Hövel P., Schöll E. Loss of coherence in dynamical networks: Spatial chaos and chimera states. *Phys. Rev. Lett.*, 2011, vol. 106, pp. 234102.
46. Omelchenko I., Riemenschneider B., Hövel P., Maistrenko Y., Schöll E. Transition from spatial coherence to incoherence in coupled chaotic systems. *Phys. Rev. E*, 2012, vol. 85, pp. 026212.
47. Hagerstrom A. M., Murphy T. E., Roy R., Hövel P., Omelchenko I., Schöll E. Experimental observation of chimeras in coupled-map lattices. *Nat. Phys.*, 2012, vol. 8, pp. 658–661.
48. Tinsley M. R., Nkomo S., Showalter K. Chimera and phase-cluster states in populations of coupled chemical oscillators. *Nat. Phys.*, 2012, vol. 8, pp. 662–665.

49. Larger L., Penkovsky B., Maistrenko Y. Virtual chimera states for delayed-feedback systems. *Phys. Rev. Lett.*, 2013, vol. 111, pp. 054103.
50. Martens E. A., Thutupalli S., Fourrière A., Hallatschek O. Chimera states in mechanical oscillator networks. *Proc. Natl. Acad. Sci. USA*, 2013, vol. 110, pp. 10563–10567.
51. Panaggio M. J., Abrams D. M. Chimera states on a flat torus. *Phys. Rev. E*, 2013, vol. 110, pp. 094102.
52. Dudkowski D., Maistrenko Y., Kapitaniak T. Different types of chimera states: An interplay between spatial and dynamical chaos. *Phys. Rev. E*, 2014, vol. 90, pp. 032920.
53. Maistrenko Y. L., Vasylenko A., Sudakov O., Levchenko R., Maistrenko V. L. Cascades of multiheaded chimera states for coupled phase oscillators. *Int J Bifurc Chaos*. 2014, vol. 24, pp. 1440014.
54. Yeldesbay A., Pikovsky A., Rosenblum M. Chimeralike states in an ensemble of globally coupled oscillators. *Phys. Rev. Lett.*, 2014, vol. 112, pp. 144103.
55. Kapitaniak T., Kuzma P., Wojewoda J., Czolczynski K., Maistrenko Y. Imperfect chimera states for coupled pendula. *Sci. Rep*., 2014, vol. 4, pp. 6379.
56. Hizanidis J., Panagakou E., Omelchenko I., Schöll E., Hövel P., Provata A. Chimera states in population dynamics: Networks with fragmented and hierarchical connectivities. *Phys. Rev. E*, 2015, vol. 92, pp. 012915.
57. Semenova N., Zakharova A., Schöll E., Anishchenko V. Does hyperbolicity impede emergence of chimera states in networks of nonlocally coupled chaotic oscillators? *Europhys. Lett.*, 2015, vol. 112, pp. 40002.
58. Olmi S., Martens E. A., Thutupalli S., Torcini A. Intermittent chaotic chimeras for coupled rotators. *Phys. Rev. E*, 2015, vol. 92, pp. 030901.
59. Panaggio M. J., Abrams D. M. Chimera states on the surface of a sphere. *Phys. Rev. E*, 2015, vol. 91, pp. 022909.
60. Kemeth F. P., Haugland S. W., Schmidt L., Kevrekidis I. G., Krischer K. A classification scheme for chimera states. *Chaos*, 2016, vol. 26, pp. 094815.
61. Schöll E. Synchronization patterns and chimera states in complex networks: Interplay of topology and dynamics. *Eur. Phys. J. Spec. Top.*, 2016, vol. 225, pp. 891–919.
62. Ulonska S., Omelchenko I., Zakharova A., Schöll E. Chimera states in networks of van der pol oscillators with hierarchical connectivities. *Chaos*, 2016, vol. 26, pp. 094825.
63. Semenova N., Zakharova A., Anishchenko V., Schöll E. Coherence-resonance chimeras in a network of excitable elements. *Phys. Rev. Lett.*, 2016, vol. 117, pp. 014102.
64. Semenov V., Zakharova A., Maistrenko Y., Schöll E. Delayed-feedback chimera states: Forced multiclusters and stochastic resonance. *Europhys. Lett.*, 2016, vol. 115, pp. 10005.
65. Hizanidis J., Kouvaris N. E., Zamora-Lòpez G., Dìaz-Guilera A., Antonopoulos C. G. Chimera-like states in modular neural networks. *Sci. Rep.*, 2016, vol. 6, pp. 19845.
66. Majhi S., Perc M., Ghosh D. Chimera states in uncoupled neurons induced by a multilayer structure. *Sci. Rep.*, 2016, vol. 6, pp. 39033.
67. Sawicki J., Omelchenko I., Zakharova A., Schöll E. Chimera states in complex networks: interplay of fractal topology and delay. *Eur. Phys. J. Spec. Top.*, 2017, vol. 226, pp. 1883–1892.
68. Rybalova E., Semenova N., Strelkova G., Anishchenko V. Transition from complete synchronization to spatio-temporal chaos in coupled chaotic systems with nonhyperbolic and hyperbolic attractors. *Eur. Phys. J. Spec. Top.*, 2017, vol. 226, pp. 1857–1866.
69. Bogomolov S. A., Slepnev A. V., Strelkova G. I., Schöll E., Anishchenko V. S. Mechanisms of appearance of amplitude and phase chimera states in ensembles of nonlocally coupled chaotic systems. *Commun. Nonlinear Sci. Numer. Simul.*, 2016, vol. 43, pp. 25–36.
70. Tian C.-H., Zhang X.-Y., Wang Z.-H., Liu Z.-H. Diversity of chimera-like patterns from a model of 2d arrays of neurons with nonlocal coupling. *Front. Phys.*, 2017, vol. 12, pp. 128904.
71. Schmidt A., Kasimatis T., Hizanidis J., Provata A., Hövel P. Chimera patterns in two-dimensional networks of coupled neurons. *Phys. Rev. E*, 2017, vol. 95, pp. 032224.
72. Shepelev I., Bukh A., Vadivasova T., Anishchenko V., Zakharova A. Double-well chimeras in 2d lattice of chaotic bistable elements. *Commun. Nonlinear Sci. Numer. Simul.*, 2018, vol. 54, pp. 50–61.
73. Hildebrand M., Cui J., Mihaliuk E., Wang J., Showalter K. Synchronization of spatiotemporal patterns in locally coupled excitable media. *Phys. Rev. E*, 2003, vol. 68, pp. 026205.
74. Kuramoto Y., Shima S.-i. Rotating spirals without phase singularity in reaction-diffusion systems. *Prog. Theor. Phys. Suppl.*, 2003, vol. 150, pp. 115–125.
75. Shima S.-i., Kuramoto Y. Rotating spiral waves with phase-randomized core in nonlocally coupled oscillators. *Phys. Rev. E*, 2004, vol. 69, pp. 036213.
76. Tang X., Yang T., Epstein I., Liu Y., Zhao Y., Gao Q. Novel type of chimera spiral waves arising from decoupling of a diffusible component. *J. Chem. Phys.*, 2014, vol. 141, pp. 024110.
77. Xie J., Knobloch E., Kao H.-C. Twisted chimera states and multicore spiral chimera states on a two-dimensional torus. *Phys. Rev. E*, 2015, vol. 92, pp. 042921.
78. Totz J. F., Rode J., Tinsley M. R., Showalter K., Engel H. Spiral wave chimera states in large populations of coupled chemical oscillators. *Nat. Phys.*, 2018, vol. 14, pp. 282–285.
79. Laing C. R. The dynamics of chimera states in heterogeneous kuramoto networks. *Physica D*, 2009, vol. 238, pp. 1569–1588.
80. Nkomo S., Tinsley M. R., Showalter K. Chimera states in populations of nonlocally coupled chemical oscillators. *Phys. Rev. Lett.*, 2013, vol. 110, pp. 244102.
81. Gu C., St-Yves G., Davidsen J. Spiral wave chimeras in complex oscillatory and chaotic systems. *Phys. Rev. Lett.*, 2013, vol. 111, pp. 134101.
82. Kuramoto Y., Shima S.-i., Battogtokh D., Shiogai Y.

Mean-field theory revives in self-oscillatory fields with non-local coupling. *Prog. Theor. Phys. Suppl.*, 2006, vol. 161, pp. 127–143.
83. Li B.-W., Dierckx H. Spiral wave chimeras in locally coupled oscillator systems. *Phys. Rev. E*, 2016, vol. 93, pp. 020202.
84. Weiss S., Deegan R. D. Weakly and strongly coupled belousov-zhabotinsky patterns. *Phys. Rev. E*, 2017, vol. 95, pp. 022215.
85. Kundu S., Majhi S., Muruganandam P., Ghosh D. Diffusion induced spiral wave chimeras in ecological system. *Eur. Phys. J. Spec. Top.*, 2018, vol. 227, pp. 983–993.
86. Guo S., Dai Q., Cheng H., Li H., Xie F., Yang J. Spiral wave chimera in two-dimensional nonlocally coupled fitzhughnagumo systems. *Chaos, Solitons & Fractals*, 2018, vol. 114, pp. 394–399.
87. Nekorkin V., Vdovin L. Map-based model of the neural activity. *Prikladnaya nelineynaya dinamika* [Applied nonlinear dynamics], 2007, vol. 15, pp. 36–60.
88. Izhikevich E. M. Which model to use for cortical spiking neurons? *IEEE Trans. Neural Netw.*, 2004, vol. 15, pp. 1063–1070.
89. Pikovsky A., Politi A. *Lyapunov Exponents*. Cambridge, Cambridge University Press, 2016. 295 p.
90. Haugland S. W., Schmidt L., Krischer K. Self-organized alternating chimera states in oscillatory media. *Sci. Rep.*, 2015, vol. 5, pp. 9883.
91. Vadivasova T. E., Strelkova G. I., Bogomolov S. A., Anishchenko V. S. Correlation analysis of the coherence-incoherence transition in a ring of nonlocally coupled logistic maps. *Chaos*, 2016, vol. 26, pp. 093108.
92. Pikovsky A., Rosenblum M., Kurths J. Synchronization: *A Universal Concept in Nonlinear Sciences*. Cambridge, Cambridge University Press, 2003. 433 p.

Cite this article as:
Bukh A. V., Strelkova G. I., Anishchenko V. S. Spiral Wave Patterns in Two-Layer 2D Lattices of Nonlocally Coupled Discrete Oscillators. Synchronization of Spiral Wave Chimeras. *Izv. Saratov Univ. (N. S.), Ser. Physics*, 2019, vol. 19, iss. 3, pp. 166–177 (in Russian). DOI: https://doi.org/10.18500/1817-3020-2019-19-3-166-177

УДК 53.01:51-73

Спирально-волновые структуры в двухслойных двумерных решетках нелокально связанных дискретных осцилляторов. Синхронизация спирально-волновых химерных состояний

А. В. Бух, Г. И. Стрелкова, В. С. Анищенко

Бух Андрей Владимирович, инженер кафедры радиофизики и нелинейной динамики, Саратовский национальный исследовательский государственный университет имени Н. Г. Чернышевского, buh.andrey@yandex.ru

Стрелкова Галина Ивановна, кандидат физико-математических наук, доцент кафедры радиофизики и нелинейной динамики, Саратовский национальный исследовательский государственный университет имени Н. Г. Чернышевского, strelkovagi@info.sgu.ru

Анищенко Вадим Семенович, доктор физико-математических наук, заведующий кафедрой радиофизики и нелинейной динамики, Саратовский национальный исследовательский государственный университет имени Н. Г. Чернышевского, wadim@info.sgu.ru

Описывается пространственно-временная динамика решетки, представляющей собой двумерную сеть нелокально связанных отображений Некоркина, моделирующих нейронную активность. Поведение сети изучается в случаях граничных условий без потока и периодических граничных условий. Показано, что в рассматриваемой решетке для определенных значений параметров связи могут наблюдаться вращающиеся спиральные волны и спирально-волновые химерные состояния. Анализируются и сравниваются статистические и динамические характеристики локальных осцилляторов из когерентных и некогерентных кластеров спирально-волнового химерного состояния. Более того, изучаются эффекты взаимной и внешней синхронизации спирально-волновых структур в двух связанных таких решетках. Численно показано, что спирально-волновые структуры, включая спирально-волновые химерные состояния, могут быть синхронизованы, и показан механизм их синхронизации. Результаты численных исследований свидетельствуют о том, что при достаточно малом значении параметра силы связи между решетками только некоторая часть осцилляторов синхронизуется, тогда как другая часть демонстрирует частично синхронное поведение. Синхронизация осуществляется для большинства осцилляторов в случае, когда пространственно-временные структуры в решетках не включают некогерентных ядер и значение параметра силы связи превышает некоторое пороговое значение. В режимах спиральнов-волновых химерных состояний режим синхронизации не достигается для всех осцилляторов, даже если значение параметра силы связи достаточно велико.

Ключевые слова: спиральные волны, спирально-волновое химерное состояние, сети, нелокальная связь, дискретное отображение, синхронизация.

Образец для цитирования:
Bukh A. V., Strelkova G. I., Anishchenko V. S. Spiral Wave Patterns in Two-Layer 2D Lattices of Nonlocally Coupled Discrete Oscillators. Synchronization of Spiral Wave Chimeras [Бух А. В., Стрелкова Г. И., Анищенко В. С. Спирально-волновые структуры в двухслойных двумерных решетках нелокально связанных дискретных осцилляторов. Синхронизация спирально-волновых химерных состояний] // Изв. Сарат. ун-та. Нов. сер. Сер. Физика. 2019. Т. 19, вып. 3. С. 166–177. DOI: https://doi.org/10.18500/1817-3020-2019-19-3-166-177